

# MITIGATION OF ELECTRON CLOUD EFFECT IN THE SuperKEKB POSITRON RING

Y. Suetsugu<sup>1,†</sup>, H. Fukuma, K. Ohmi, M. Tobiyama<sup>1</sup>, H. Ikeda<sup>1</sup>, K. Shibata<sup>1</sup>, T. Ishibashi<sup>1</sup>, M. Shirai,  
S. Terui, K. Kanazawa, H. Hisamatsu, M. L. Yao<sup>1</sup>, KEK, Tsukuba, Japan  
<sup>1</sup>also at SOKENDAI, Hayama, Japan

## Abstract

A critical issue for SuperKEKB is the electron cloud effect (ECE) in the positron ring. Various countermeasures, such as ante-chambers, TiN-film coatings, clearing electrodes, and grooved surfaces, were prepared before commencing commissioning. The ECE, however, was observed during Phase-1 commissioning (2016) caused by the electron cloud in Al-alloy bellows chambers and also in the beam pipes at drift spaces, although the beam pipes had antechambers and TiN-film coatings. The threshold of the current linear density for exciting the ECE was approximately 0.12 mA bunch<sup>-1</sup> RF-bucket<sup>-1</sup>. Permanent magnets and solenoids were attached to them to generate magnetic fields in the beam direction as additional countermeasures. Consequently, the current linear density threshold increased up to over 0.53 mA bunch<sup>-1</sup> RF-bucket<sup>-1</sup> in Phase-3 commissioning (2019). Currently, there is no clear evidence of ECE during a normal operation. The effectiveness of the ante-chambers and TiN-film coatings of real beam pipes and groove structures used in bending magnets were experimentally re-evaluated. This report summarises the mitigation techniques used in SuperKEKB and the results thus far.

## INTRODUCTION

The SuperKEKB is an electron-positron collider with asymmetric energies in KEK that aims for an extremely high luminosity utilising a “nano-beam” collision scheme (Fig. 1) [1, 2]. The main ring (MR) consists of two rings, that is, the high-energy ring (HER) for 7 GeV electrons and the low-energy ring (LER) for 4 GeV positrons. The beam pipes in the MR tunnel are shown in Fig. 2.



Figure 1: SuperKEKB at KEK Tsukuba campus.

<sup>†</sup> yusuke.suetsugu@kek.jp

Single-bunch instability caused by the electron cloud, that is, the electron cloud effect (ECE), is a severe problem for the SuperKEKB LER [3, 4]. Therefore, more effective countermeasures are required. From simulations, the average density of electrons in the ring should be less than  $\sim 3 \times 10^{11} \text{ m}^{-3}$  to avoid excitation of the ECE [5]. Hence, various types of countermeasures against ECE were adopted in the SuperKEKB LER, which are summarized in Table 1, and typical views of each countermeasure are shown in Fig. 3 [6].

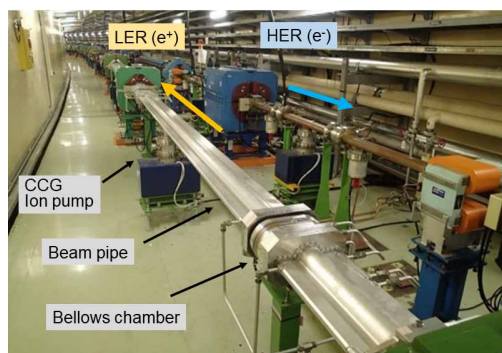


Figure 2: LER and HER in the MR tunnel.

## COUNTERMEASURES IN SUPERKEKB

An antechamber helps to minimise the effects of photoelectrons because most of the synchrotron radiation (SR) is directly irradiated at its side wall (Fig. 3(a)). However, secondary electrons play a significant role in electron cloud formation in the high-bunch current regime. Most of the beam pipes for the LER were made of aluminium (Al)-alloy, and the beam channel was coated with a TiN film to reduce the secondary electron yield (SEY) (Fig. 3(b)). Clearing electrodes were installed in the beam pipes for wiggler magnets instead of TiN-film coating. A clearing electrode absorbs electrons around the beam orbit using a static electric field. These beam pipes also have antechambers and are made of copper (Fig. 3(c)). A grooved surface was adopted for the beam pipes in the bending magnets in the arc section. The grooved surface geometrically reduces the SEY. The TiN-film coating was subsequently applied to the grooved surface (Fig.3(d)). As a result, approximately 90% of the beam pipes in the ring had antechambers and TiN-film coating. A magnetic field in the beam direction ( $B_z$ ) generated by solenoids or permanent magnets around the beam pipe is highly effective in suppressing the electron emissions from the inner wall. These are available only in the drift spaces (field-free regions) between electromagnets, such as quadrupole and sextupole magnets (Fig.3(e) and 3(f)). The circular dots in Table 1 indicate the

Table 1: Countermeasures used to minimize the ECE in the SuperKEKB LER. The circular dots indicate the countermeasures applied for each main section in the ring.

Sections	Length [m]	$n_e$ (circular) [m <sup>-3</sup> ]	Antechamber (1/5)	TiN coating (3/5)	Solenoid ( $B_z$ ) (1/50)**	Groove (1/2)	Electrode (1/100)	$n_e$ (expected) [m <sup>-3</sup> ]
Drift space (arc)	1629	$8 \times 10^{12}$	•	•	•			$2 \times 10^{10}$
Corrector mag.	316	$8 \times 10^{12}$	•	•	•			$2 \times 10^{10}$
Bending mag.	519	$1 \times 10^{12}$	•	•		•		$6 \times 10^{10}$
Wiggler mag.	154	$4 \times 10^{12}$	•	•*			•	$5 \times 10^9$
Quadrupole and Sextupole mag.	254	$4 \times 10^{10}$	•	•				$5 \times 10^9$
RF cav. section	124	$1 \times 10^{11}$		•	•			$1 \times 10^9$
IR	20	$5 \times 10^{11}$		•	•			$6 \times 10^9$
Total	3016							
Average		$5.5 \times 10^{12}$						$2.4 \times 10^{10}$

\*Except for beam pipes with clearing electrodes.

\*\*Uniform magnetic field in the beam direction is assumed.

Abbreviations:

RF cav. section: Beam pipes around RF cavities, IR: Interaction region

$n_e$  (circular): Density of electrons expected for circular beam pipe (copper)

$n_e$  (expected): Density of electrons expected after applying countermeasures

Antechamber: Antechamber scheme, Solenoid: Solenoid winding, but actually applying a magnetic field in the beam direction ( $B_z$ )

Groove: Beam pipe with grooves, Electrode: Beam pipe with clearing electrodes

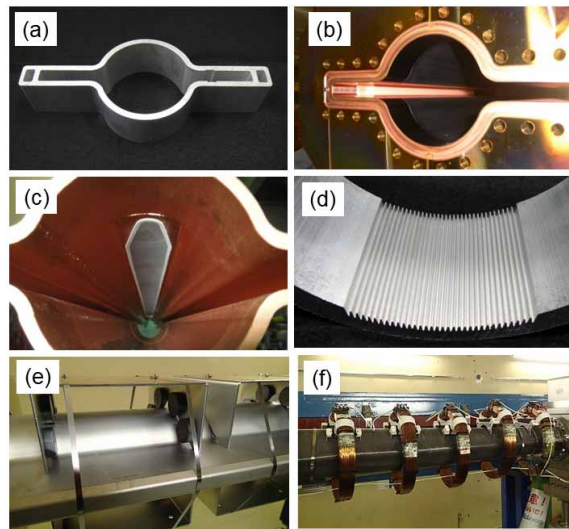


Figure 3: Typical view of countermeasures adopted to SuperKEKB LER: (a) beam pipes with ante-chambers, (b) TiN-film coating, (c) clearing electrode, (d) groove structure, magnetic fields in the beam direction by (e) permanent magnets, and (f) solenoids.

countermeasures applied to each main section of the ring. The density of electrons ( $n_e$ ) expected in the case of circular beam pipes (copper) and those with the above countermeasures are also presented in the table. Here, the efficiencies in reducing  $n_e$  for the antechamber scheme, TiN-film coating, solenoid (i.e.,  $B_z$ ), grooved surface, and clearing electrode are assumed to be 1/5, 3/5, 1/50, 1/2, and 1/100, respectively, based on the experimental results obtained in the R&D up to that time. With these countermeasures, a  $n_e$

value of approximately  $2 \times 10^{10} \text{ m}^{-3}$  was expected at the designed beam parameters, that is, a beam current of 3.6 A at a bunch fill pattern of one train of 2500 bunches, with a bunch spacing of two RF-buckets (referred to as 1/2500/2 RF hereafter). Here, one RF-bucket corresponds to 2 ns. This value of  $n_e$  is sufficiently lower than the threshold density of electrons ( $n_{e,th}$ ) of  $3 \times 10^{11} \text{ m}^{-3}$ . The  $B_z$  at drift spaces were not prepared before Phase-1 commissioning because the expected beam current was not very high during the Phase-1 commissioning; it was approximately a maximum of 1 A.

Several beam pipes for tests were installed in the ring to investigate ECE, and the  $n_e$  around the beam was measured via electron current monitors, which were also used in previous KEKB experiments [7]. A test beam pipe with two electron monitors is shown in Fig. 4. These monitors were set up at the bottom of the beam channel. The voltage applied to the electron collector was 100 V, whereas that applied to the grid (repeller) was typically -500 V. The test beam pipe is placed in the arc section of the ring. The line density of synchrotron radiation (SR) photons is  $1 \times 10^{15} \text{ photons s}^{-1} \text{ m}^{-1} \text{ mA}^{-1}$ , which is almost the same as the average value of the arc sections. A weak magnetic field in the vertical direction ( $B_y$ ) can be applied at the location of the electron monitors by the solenoids at the top and bottom sides of the beam pipe (see Fig. 4).

## ECE IN PHASE-1 COMMISSIONING

### First Observation

ECEs, such as a blow-up of vertical beam size and non-linear pressure rise with beam current, were first observed during Phase-1 commissioning from a beam current ( $I$ ) of approximately 600 mA at a bunch fill pattern of

Content from this work may be used under the terms of the CC-BY-4.0 licence (© 2022). Any distribution of this work must maintain attribution to the author(s), title of the work, publisher, and DOI

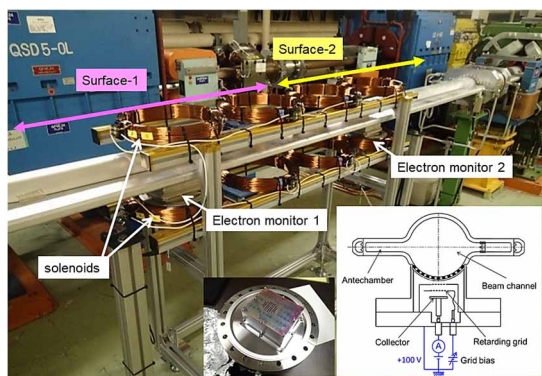


Figure 4: A test beam pipe with two electron monitors installed at a drift space of the LER.

1/1576/3.06 RF, despite the implementation of the various countermeasures described above [8, 9]. Here “3.06RF” means the average RF-bucket spacings of a pattern with a mixture of 3 and 4 RF-bucket spacings. This value of  $I$  corresponds to the current line density ( $I_d$ ), i.e., the bunch current divided by the bunch spacing, of  $0.12 \text{ mA bunch}^{-1} \text{ RF-bucket}^{-1}$ . The vertical beam size was measured using an X-ray beam size monitor [10]. Since  $B_z$  was not applied to the beam pipes at the drift spaces, the excitation of the ECE is an undeniable possibility. However, the threshold of the beam current for exciting the ECE was much lower than expected, that is, over 1 A with 3RF-bucket spacings.

A dedicated machine study to investigate the phenomena found that the threshold of  $I_d$  ( $I_{d,th}$  [ $\text{mA bunch}^{-1} \text{ RF-bucket}^{-1}$ ]) where the blow-up of the beam size begins was almost independent of the bunch fill patterns, as shown in Fig. 5(a). This is a typical characteristic of ECE. The  $I_{d,th}$  was  $0.1 - 0.12 \text{ mA bunch}^{-1} \text{ RF-bucket}^{-1}$ . The modes of coupled-bunch instability were also typical for ECE because of the electrons in the drift spaces [11]. Furthermore, the  $n_e$  measured at the region “without” TiN-film coating in the test beam pipe was of the order of  $10^{12} \text{ m}^{-3}$  at an  $I$  value of 600 mA. The  $n_e$  value was over 10 times higher than  $n_{e,th}$ ,  $\sim 3 \times 10^{11} \text{ m}^{-3}$ , as expected from the simulation. It was observed that this ECE was caused by the electrons in the Al-alloy bellows chambers without TiN-film coating (see Fig. 2), although they occupy only  $\sim 5\%$  of the circumference of the ring.

To counteract the ECE, two units of permanent magnets (PM), where eight small ( $\phi = 30 \text{ mm}$ ) PMs were attached to a C-shaped iron plate (yoke) in each unit, were placed at the top and bottom of each Al-alloy bellows chamber, as shown in Fig. 6. A  $B_z$  value of approximately 100 G was formed in most regions of the PM units, although the polarity reverses locally near the magnets.

### ECE at a Higher Beam Current

After attaching the PM units to all the Al-alloy bellows chambers, the blow-up of the vertical beam size was not evident until  $I$  reached  $\sim 800 \text{ mA}$ . The measurement of the vertical beam size for bunch fill patterns of 4/150/2 RF, 4/150/3 RF, 4/150/4 RF and 4/150/6 RF showed that the

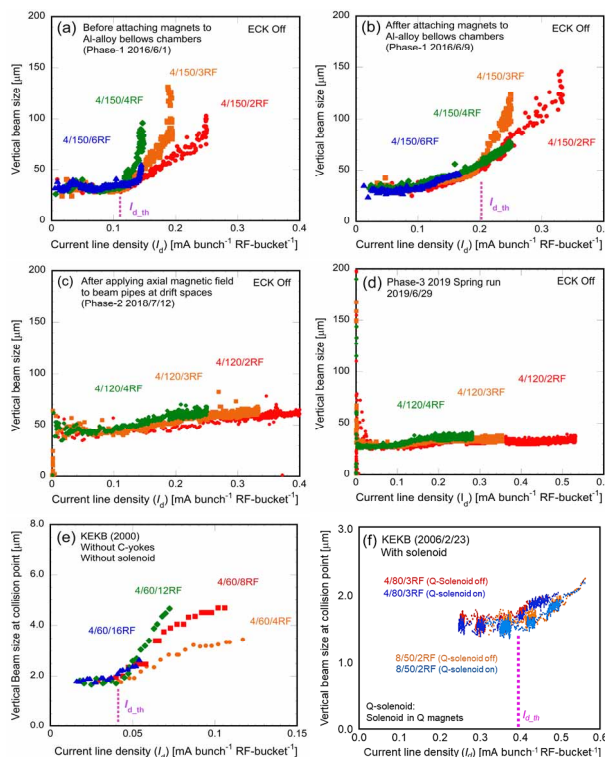


Figure 5: Vertical beam sizes as a function of the current line density ( $I_d$ ) for several bunch fill patterns measured (a) before and (b) after attaching PM units to Al-alloy bellows chambers in Phase-1 commissioning, (c) in Phase-2 commissioning, (d) in Phase-3 commissioning, and in the KEKB era (e) without and (f) with solenoids, where ECK means the emittance control knob.

$I_{d,th}$  shifted from  $0.12 \text{ mA bunch}^{-1} \text{ RF-bucket}^{-1}$  to approximately  $0.2 \text{ mA bunch}^{-1} \text{ RF-bucket}^{-1}$ , as shown in Fig. 5(b).

The  $n_e$  measured in the region “with” TiN-film coating in the test beam pipe approached the value of  $n_{e,th}$  at the  $I_d$  of  $0.2 \text{ mA bunch}^{-1} \text{ RF-bucket}^{-1}$ . Transverse coupled bunch instabilities with modes caused by electrons in drift spaces were also detected. This means that ECE was excited by the electron cloud formed in the beam pipes with antechambers and TiN-film coating at the drift spaces.

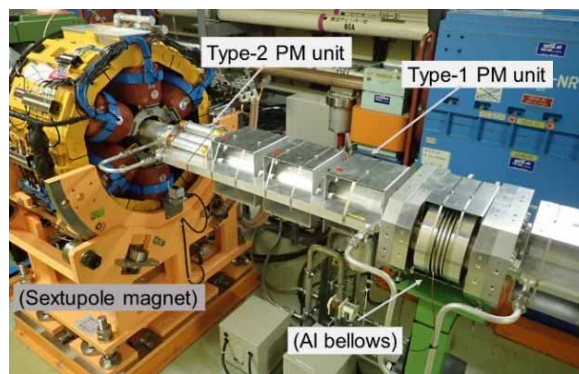


Figure 6: PM units attached to the beam pipes at drift spaces.

At this point, approximately 90 % of the beam pipes in the LER had antechambers and TiN-film coating. It should be noted that  $I_{d,th}$  is much higher than that in the case of the KEKB at an early stage [12], where most beam pipes were circular and made of copper (OFHC) without any coatings or solenoid windings. The  $I_{d,th}$  at that time was approximately  $0.04 \text{ mA bunch}^{-1} \text{ RF-bucket}^{-1}$ , as shown in Fig. 5(e). Meanwhile, after applying PM units to only Al-alloy bellows chambers in the SuperKEKB, the  $I_{d,th}$  is  $0.2 \text{ mA bunch}^{-1} \text{ RF-bucket}^{-1}$  (Fig. 5(b)), which is approximately five times that in the KEKB. This indicates that the antechambers and TiN-film coating of the beam pipes effectively suppressed the ECE.

### Additional countermeasures

PM units and solenoids were attached to most of the beam pipes at drift spaces in the LER as additional countermeasures for the next Phase-2 commissioning phase. The PM units with iron yokes (Type-1 unit), similar to those used for Al-alloy bellows chambers, were placed in series around the beam pipe, as shown in Fig. 6, which produced a  $B_z$  of approximately 60 G. A simulation using the CLOUDLAND code [13] showed that  $n_e$  around the beam orbit reduced to approximately 1/10th of  $n_{e,th}$  even for the designed beam parameters, as shown in Figs. 7(a) and 7(b). However, Type-1 units cannot be used near electromagnets, such as quadrupole and sextupole magnets, because the iron yokes affect their magnetic fields. Therefore, another type of PM unit (Type-2 unit), consisting of Al-alloy cylinders with permanent magnets inside and Al-alloy supports, was placed close to the electromagnets (Fig. 6). The value of  $B_z$  inside the Type-2 unit was approximately 100 G. Solenoid windings were revived for the beam pipes that had been used since the KEKB era [14]. Before starting Phase-2 commissioning, as a result, approximately 86% of the drift spaces (approximately 2 km) were covered with a  $B_z$  higher than approximately 20 G. A simulation indicated that the  $n_e$  around the beam orbit at a  $B_z$  value higher than 10 G is lower than  $1 \times 10^{11} \text{ m}^{-3}$  even for the designed beam parameters [6].

## ECE IN PHASE-2 COMMISSIONING

Figure 5(c) shows the dependence of the vertical beam size on  $I_d$  for the three bunch fill patterns in Phase-2 commissioning, 2018. The blow-up of the beam sizes was not observed until the  $I_d$  of  $0.4 \text{ mA bunch}^{-1} \text{ RF-bucket}^{-1}$ .  $I_{d,th}$  increased by at least two times compared to Phase-1 commissioning (Fig. 5(b)).  $I_d$  is the maximum value that can be stably stored at that time. The pressure increased in almost proportionally with the beam current.

The modes and growth rates of the transverse coupled bunch instabilities were measured and analysed again. The modes caused by the electrons near the inner wall trapped by  $B_z$  were observed, instead of the modes caused by the electrons in the drift spaces [15]. Furthermore, the growth rates were much slower than those measured during Phase-1 commissioning. The coupled bunch instability

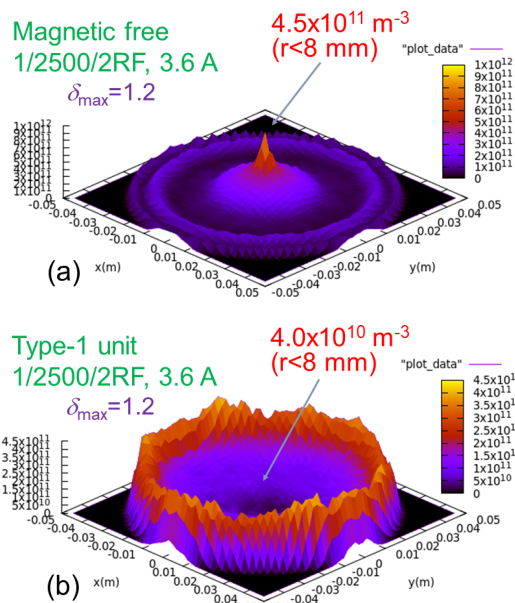


Figure 7: Density of electrons ( $n_e$ ) in a beam pipe (a) without magnetic field and (b) with Type-1 PM units calculated by CLOUDLAND simulation code for a beam current of 3.6A at a bunch fill pattern of 1/2500/2RF.

was effectively suppressed by the bunch-by-bunch feedback system. The measured  $n_e$  in the test beam pipe in the region with TiN-film coating without  $B_z$  did not change from that observed in Phase-1 commissioning.

From these observations, it can be concluded that additional countermeasures, that is, a  $B_z$  generated by PM units and solenoids at drift spaces, contributed to suppressing the ECE in Phase-2 commissioning.

### Re-evaluation of the Effectiveness of Antechamber and TiN-film Coating

First, as a measure of the effectiveness of a beam pipe with an antechamber in suppressing photoelectrons, the reduction rate of the number of photoelectrons in the beam channel relative to a simple circular beam pipe ( $\alpha$ ) is defined as follows:

$$\alpha \equiv \frac{p_b + \beta \times p_a}{p_b + p_a} \quad (1)$$

Here,  $p_b$  and  $p_a$  are the numbers of photoelectrons generated in the beam channel and antechamber, respectively. Hence, the total number of photoelectrons in the beam pipe at this location is  $p_b + p_a$ .  $\beta$  is the probability that the electrons in the antechamber pass into the beam channel and is estimated to be approximately 0.05 in our case through a simulation [6]. For the case of a circular beam pipe, for example,  $\alpha = 1$  because  $\beta = 1$ . A small value of  $\alpha$  implies the high effectiveness of the antechamber.

Meanwhile, the maximum SEY ( $\delta_{max}$ ) was used as a measure of the effectiveness of TiN-film coating with regards to reducing secondary electrons.  $\delta_{max}$  was estimated using the fact that the ECE was excited at an  $I$  value of

Content from this work may be used under the terms of the CC-BY-4.0 licence (© 2022). Any distribution of this work must maintain attribution to the author(s), title of the work, publisher, and DOI

approximately 900 mA for a bunch fill pattern of 1/1576/3.06 RF during Phase-1 commissioning as described previously. This implies that  $n_e$  should be approximately  $3 \times 10^{11} \text{ m}^{-3}$  for these beam parameters. The line density of photons of SR is  $1 \times 10^{15} \text{ photons s}^{-1} \text{ m}^{-1} \text{ mA}^{-1}$  on average in the beam pipes at the arc sections. Under these conditions,  $\delta_{max}$  was calculated as a function of the number of photoelectrons in the beam channel, that is,  $\alpha$ , using CLOUDLAND and PyECLOUD [16] simulation codes.

If the value of  $\alpha$  is estimated from simulations or measurements,  $\delta_{max}$  of the surface can be evaluated. For example, the value of  $\alpha$  was estimated to be 0.01 in the experiment during the KEKB commissioning, where a test beam pipe with an antechamber made of pure copper was used [17]. Using this  $\alpha$  value,  $\delta_{max}$  was estimated to be approximately 1.4. This value of  $\delta_{max}$  is higher than that obtained for TiN-film coating (1.0 – 1.2) after sufficient electron bombardment in a laboratory [18]. Hence, estimating the  $\alpha$  value for a real beam pipe is necessary.

Note that the re-evaluated values of  $\alpha$  and  $\delta_{max}$  here are the averages of those measured in the ring because the ECE is excited by the average value of  $n_e$ . However, ~90% of the beam pipes in the ring have antechambers and TiN-film coating. Beam pipes in other parts do not have antechambers but are in straight sections with weak SR intensity. The effects of these parts are small.

$\alpha$  and  $\delta_{max}$  values were re-evaluated by several methods using simulations and experiments during Phase-2 commissioning [6]. Here, the result obtained from the measured  $n_e$  with small permanent magnets at the ends of antechambers is reported as a representative example.

If  $n_e$  is almost proportional to the number of photoelectrons in the beam channel, which holds for the  $n_e$  value of the order of  $10^{11} \text{ m}^{-3}$ , the ratio of electron density under the condition that the electrons from the antechamber can be negligible ( $n_{e0}$ ) to that under the usual condition ( $n_e$ ) is written as follows:

$$\frac{n_{e0}}{n_e} = \frac{p_b}{p_b + \beta \times p_a} \quad (2)$$

If  $n_{e0}$  and  $n_e$  are measured, then the  $\alpha$  value can be deduced using Eqs. (1) and (2).

$n_{e0}$  was measured during Phase-2 commissioning by attaching weak permanent magnets with yokes at only the ends of the antechambers along the test beam pipe, as shown in Fig. 8. These magnets generate weak  $B_y$  along the antechamber and confine the emitted photoelectrons. The  $B_y$  value close to the permanent magnets, that is, at the end of the antechamber, was approximately 100 G, but that in the beam channel was less than 0.5 G, which is the same order as the terrestrial magnetism. In the simulation, a  $B_y$  of this order of magnitude had no effect on  $n_e$  in the beam channel. It was also experimentally found to have little effect on the measurement of  $n_e$  using our electron monitors.

The measured values of  $n_{e0}$  and  $n_e$  for a bunch fill pattern of 1/1576/3.06 RF are presented in Fig. 9. High  $n_e$  values at low  $I_d$  are not reliable because the volume used in the

calculation of  $n_e$  is so small that the estimation method is no longer valid in principle [7]. The ratio  $n_{e0}/n_e$  was 1.5/3.3 at a bunch current of 0.45 mA bunch<sup>-1</sup>. Assuming a  $\beta$  value of 0.05, the ratio  $p_b/p_a$  was calculated to be 0.04 from Eq. (2).  $\alpha$  was then calculated as 0.08 from Eq. (1). Consequently,  $\delta_{max}$  was evaluated to be approximately 0.7 – 0.8, which is close to the value obtained in the laboratory.

Although the results of the re-evaluation studies were relatively scattered, all values of  $\alpha$  were larger than that obtained in the KEKB experiments, that is, 0.01 [6]. This difference can be explained by the following: (a) the location of the experimental setup, that is, just downstream (KEKB) and seven meters downstream (SuperKEKB) of a bending magnet, (b) the height of the antechamber, that is, 18 mm (KEKB) and 14 mm (SuperKEKB), (c) the material of the beam pipe, that is, copper (KEKB) and Al-alloy (SuperKEKB), and (d) the treatment of the innermost surface of the antechamber where the SR is directly irradiated. The most plausible cause among these is (a) and (b); that is, some portion of photons from upstream hit the beam channel owing to the vertical spread and scattering far downstream of the bending magnets in the real machine.

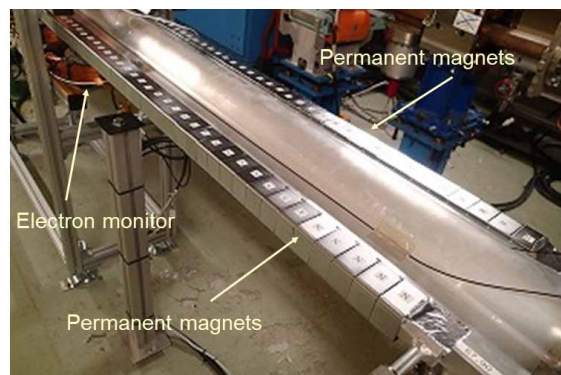


Figure 8: Weak PMs attached at the ends of antechambers of the test beam pipe with electron monitors to prevent the photoelectrons generated in the antechamber from entering the beam channel.

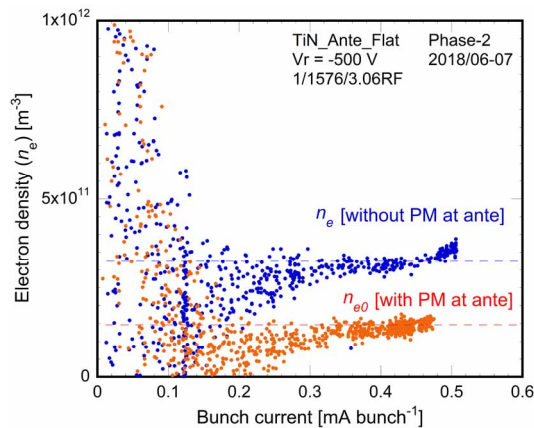


Figure 9: Measured electron density near the beam orbit for the cases with ( $n_{e0}$ ) and without PMs ( $n_e$ ) in the antechambers.

Conversely, for the  $\delta_{max}$  of the TiN-film coating, the values are closer to or are somewhat lower than those obtained in the laboratory. The TiN-film coating seems to work well as expected, with regards to reducing the emission of secondary electrons.

### ECE IN PHASE-3 COMMISSIONING

Before starting Phase-3 commissioning, the PM units were further added to the drift spaces, up to approximately 91% of the drift spaces. During Phase-3 commissioning in June 2019, the vertical beam sizes and modes of instabilities were again measured by changing the bunch fill patterns. The changes in the vertical beam sizes with respect to  $I_d$  for the bunch fill patterns of 4/120/2 RF, 4/120/3 RF and 4/120/4 RF are shown in Fig. 5(d). No beam-size blow-up was observed until the  $I_d$  of 0.53 mA bunch<sup>-1</sup> RF-bucket<sup>-1</sup>, which was approximately 2.6 times higher than that in Phase-1 commissioning. Note again that  $I_d$  is the maximum value that can be stably stored at that time. Furthermore, coupled-bunch instabilities related to the electron cloud in the drift spaces were not observed. The pressure increased almost proportionally to the beam current, and no abnormal pressure increases were observed. The  $B_z$  produced by the PMs works effectively to suppress ECE. The  $I_d$  of 0.53 mA bunch<sup>-1</sup> RF-bucket<sup>-1</sup> corresponds to approximately 2.5 A for the bunch fill pattern of 1/2400/2 RF.

As a reference, the changes in vertical beam sizes against  $I_d$  for the bunch fill patterns of 4/80/3 RF and 8/50/2 RF after setting solenoids in the KEKB era (2006) are shown in Fig. 5(f) [19], where most of the drift spaces and the beam pipes in quadrupole magnets were covered with solenoids. The condition regarding the magnetic fields in the beam direction is similar to that in Phase-3 of SuperKEKB. The  $I_{d,th}$  was approximately 0.4 mA bunch<sup>-1</sup> RF-bucket<sup>-1</sup> at that time. After this measurement, the  $B_z$  of approximately 1500 solenoids was increased by a factor of 1.7 with new power supplies, and the  $I_{d,th}$  should have somewhat improved [20]. A measurement showed that the value of  $I_{d,th}$  was 0.44 mA bunch<sup>-1</sup> RF-bucket<sup>-1</sup> at a bunch fill pattern of 8/100/2 RF in June 2009.

The effectiveness of the groove structure on the top and bottom sides of the beam channel was also re-evaluated. As for the groove structure, the effects on the reduction of SEY were examined in the KEKB era at a wiggler section by changing the shape and materials of the groove structures [21]. The effectiveness was evaluated using a test chamber with the same groove structure used for the beam pipes in the bending magnets of SuperKEKB [22]. Figure 10(a) and 10(b) show the dependence of the measured electron current ( $I_e$ ) on the beam current ( $I$ ) for the bunch fill pattern of 1/1576/3.05 RF at  $B_y = 0$  in the test chamber. The value of  $I_{e\_Al}$  (without groove and TiN-film coating) was much higher than that of the  $I_{e\_Al+groove}$  (with groove but without TiN-film coating), and the effectiveness of the groove structure was evident. However, the values of  $I_{e\_TiN}$  (without groove but with TiN-film coating) and  $I_{e\_TiN+groove}$  (with both groove and TiN-film coating) are almost identical. The possible reasons for this are as follows. The value of

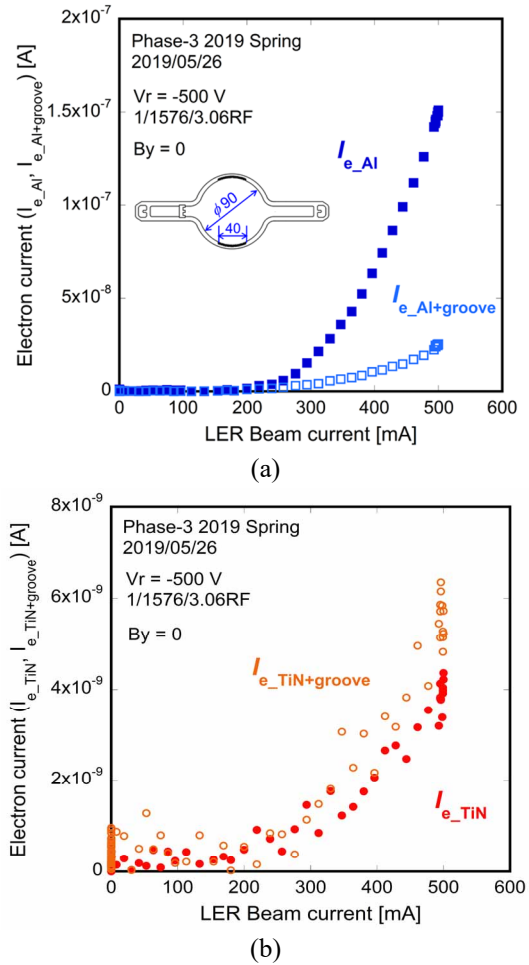


Figure 10: Electron currents of Al-alloy beams pipes (a) without and (b) with TiN-film coating for without ( $I_{e\_Al}$ ,  $I_{e\_TiN}$ ) and with ( $I_{e\_Al+groove}$ ,  $I_{e\_TiN+groove}$ ) groove structure in each case ( $B_y = 0$ ).

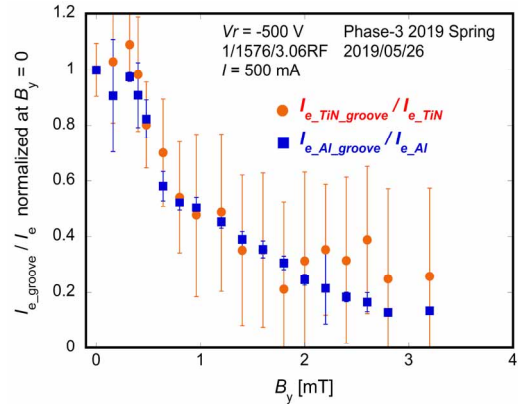


Figure 11: Changes of  $I_{e\_TiN+groove} / I_{e\_TiN}$  and  $I_{e\_Al+groove} / I_{e\_Al}$  against  $B_y$ , where the values are normalized at  $B_y = 0$ .

$n_e$  in the beam pipe with the TiN-film coating (low SEY) was of the order of  $10^{11} \text{ m}^{-3}$ , and the effect of photoelectrons was larger than that of secondary electrons. Therefore,  $I_e$  is almost the same regardless of the presence or absence of groove structures. In contrast, for the case without the

Content from this work may be used under the terms of the CC-BY-4.0 licence (© 2022). Any distribution of this work must maintain attribution to the author(s), title of the work, publisher, and DOI

Content from this work may be used under the terms of the CC-BY-4.0 licence (© 2022). Any distribution of this work must maintain attribution to the author(s), title of the work, publisher, and DOI

TiN-film coating (high SEY), the value of  $n_e$  is of the order of  $10^{12} \text{ m}^{-3}$ , and the SEY plays a large role. The effect of the groove structure with a low SEY was clearly observed.

Considering the positions of the groove structures, that is, the top and bottom of the beam channel, as shown in Fig. 10(a),  $I_e$  was measured by applying a weak  $B_y$  at the location of the electron monitors. It is expected that the effect of the groove structure becomes prominent when restricting the movement of electrons in the vertical direction by applying  $B_y$ . Furthermore, photoelectrons from the side of the beam pipes are suppressed. However, estimating  $n_e$  becomes impossible using the method used so far. The dependences of  $I_{e\_Al+groove}/I_{e\_Al}$  and  $I_{e\_TiN+groove}/I_{e\_TiN}$  on  $B_y$  at  $I = 500 \text{ mA}$  are plotted in Fig. 11. Here, the measured values were normalised to the values of  $B_y = 0$  to observe qualitative changes. Despite the scattering of the measured values for the case of the TiN-film coating, the measured  $I_e$  with the groove structure ( $I_{e\_Al+groove}$  and  $I_{e\_TiN+groove}$ ) became smaller than those without it ( $I_{e\_Al}$  and  $I_{e\_TiN}$ ) with  $B_y$ . This means that the SEY of the groove structure is smaller than that of the smooth surfaces, regardless of the presence or absence of TiN-film coating. Beam pipes with a groove structure are used in bending magnets, and the results obtained here also hold in the real case.

Since the experiment in 2019, we have had little chance to conduct dedicated experiments on ECE using a single beam. As a piece of supporting evidence that the ECE causes no beam size blow-up during the physics run (colliding beams), the luminosity of each bunch at a bunch fill

pattern of 2/1173/2.04 RF measured by the zero-degree luminosity monitor (ZDLM) [23] at a beam current of 1250 mA in June 2022 is shown in Fig. 12 (corresponding to the  $I_d$  of approximately  $0.26 \text{ mA bunch}^{-1} \text{ RF-bucket}^{-1}$ ). Currently, almost all the parts of the trains are two RF-bucket spacings. As seen in the figure, the bunch luminosity seems to be flat along the train, and there is no apparent "long-term" change for each train. The reasons for the high hit rate at the beginning of each bunch train (i.e., bunch number of 1–15 and 2561–2575 in Fig. 12) are the effects of the dead time and pile-up of the detector, non-uniformity of the bunch current, and beam-beam effects, although further analysis is required [24]. As indicated in this figure, there is no degradation in the luminosity along the train, which is a result of the beam-size blow-up caused by the ECE.

In the recent single-beam operation, a vertical beam-size blow-up was observed at a bunch current of approximately  $0.6 \text{ mA bunch}^{-1}$ , independent of bunch fill patterns [2]. A coherent oscillation at the frequency corresponding to  $\nu_y - \nu_s$  was observed, and this instability was called “-1 mode instability”, where  $\nu_y$  and  $\nu_s$  are the vertical betatron and synchrotron tunes, respectively. The instability is not caused by ECE, but is related to the impedance, especially that of the beam collimators. Further investigation is required to understand the instability mechanism.

As a part of R&D, to search for a surface with a lower SEY than before, a surface with thermal-sprayed copper has been investigated in the laboratory [25]. The rough surface geometrically decreases the SEY. The  $\delta_{max}$  was approximately 0.7, even without TiN-film coatings, after sufficient electron bombardment. During Phase-3 commissioning, a test beam pipe with this surface was first installed in the ring, and its properties were studied using beams. The measured  $n_e$  value was lower than that of the surface with the TiN-film coating (2/1124/2.13 RF). Further analysis of these results is underway.

## SUMMARY

ECE was observed in the SuperKEKB LER during Phase-1 commissioning. The ECE due to the Al-alloy bellows chambers and the beam pipes at drift spaces was successfully suppressed by applying PM units which produced a  $B_z$  of  $\sim 60 \text{ G}$ . The antechambers and TiN-film coating seemed to function to some extent, but the experiment during Phase-2 commissioning found that the effectiveness of the antechambers of the real beam pipe in suppressing the photoelectron was lower than expected. The importance of suppressing photoelectrons was recognized. In the experiment in Phase-3 commissioning, no beam size bow-up was observed until the  $I_d$  of  $0.53 \text{ mA bunch}^{-1} \text{ RF-bucket}^{-1}$ . The effectiveness of the groove structure adopted in the real ring in decreasing the SEY was also confirmed. It is deduced from the bunch-by-bunch luminosity measurement that there is no beam-size blow-up in the usual operation condition until a beam current of 1250 mA with a bunch fill pattern of 2/1173/2.04 RF in June, 2022.

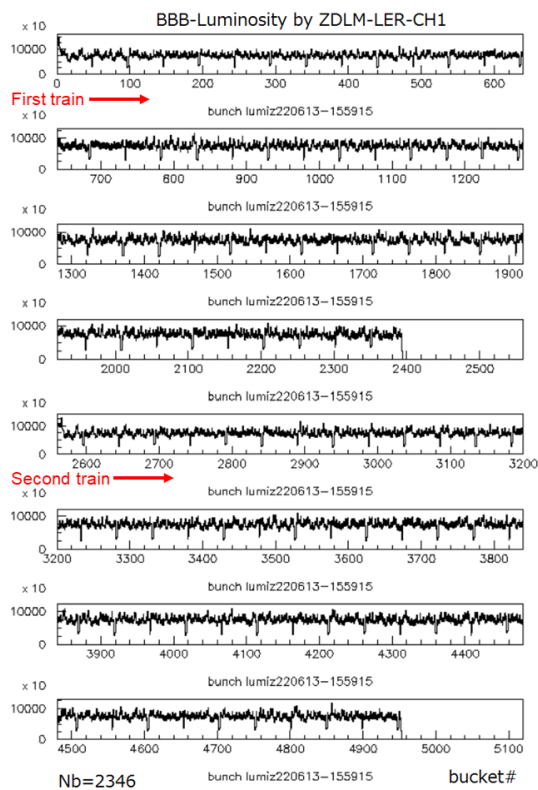


Figure 12: Bunch-by-bunch luminosity for a bunch fill pattern of 2/1173/2.04RF on 13<sup>th</sup> June, 2022. The vertical axis shows the number of hits at the ZDLM channel.

SuperKEKB continues the physics experiment. The luminosity has been increasing annually, breaking the world record since 2021. No indication of ECE has been observed, and the various countermeasures against ECE seem to be working as expected. However, the design beam current (corresponding to an  $I_d$  of 0.73 mA bunch<sup>-1</sup> RF-bucket<sup>-1</sup>) has not yet been achieved. Careful observations of the ECE will continue during Phase-3 commissioning and beyond.

## ACKNOWLEDGEMENTS

The authors would like to thank all the staff of the KEKB accelerator division for their cooperation and continuous encouragement during the commissioning phase.

## REFERENCES

- [1] SuperKEKB, <https://www-superkekb.kek.jp/>.
- [2] Y. Funakoshi *et al.*, “The SuperKEKB has Broken the World Record of the Luminosity”, in *Proc. IPAC’22*, Bangkok, Thailand, Jun. 2022, pp. 1–5.  
doi: 10.18429/JACoW-IPAC2022-MOPLXGD1
- [3] K. Ohmi and F. Zimmermann, “Head-Tail Instability Caused by Electron Clouds in Positron Storage Rings”, *Phys. Rev. Lett.*, vol. 85, p. 3821, 2000.  
doi:10.1103/PhysRevLett.85.3821
- [4] F. Zimmermann, “Review of single-bunch instabilities driven by an electron cloud”, *Phys. Rev. ST Accel. Beams*, vol. 7, p. 124801, 2004.  
doi:10.1103/PhysRevSTAB.7.124801
- [5] Y. Susaki and K. Ohmi, “Electron cloud instability in SuperKEKB low energy ring,” in *Proc. IPAC’10*, Kyoto, May 2010, pp.1545–1547, <https://accelconf.web.cern.ch/IPAC10/papers/tupeb014.pdf>
- [6] Y. Suetsugu *et al.*, “Mitigating the electron cloud effect in the SuperKEKB positron ring”, *Phys. Rev. Accel. Beams*, vol. 22, p. 023201, 2019.  
doi:10.1103/PhysRevAccelBeams.22.023201
- [7] K. Kanazawa *et al.*, “Measurement of the electron cloud density around the beam”, in *Proc. PAC’05*, Knoxville, USA, May 1995, pp. 1054–1056, <https://accelconf.web.cern.ch/p05/PAPERS/FPAP007.PDF>
- [8] Y. Suetsugu *et al.*, “Achievements and problems in the first commissioning of SuperKEKB vacuum system”, *J. Vac. Sci. Technol. A*, vol. 35, p. 03E103, 2017.  
doi:10.1116/1.4977764
- [9] Y. Suetsugu *et al.*, “First Commissioning of the SuperKEKB Vacuum System”, *Phys. Rev. Accel. Beams*, vol. 19, p. 121001, 2016.  
doi:10.1103/PhysRevAccelBeams.19.121001
- [10] E. Mulyani, *et al.*, “Image Reconstruction Techniques Based on Coded Aperture Imaging for SuperKEKB X-Ray Beam Size Monitor”, in *Proc. IPAC’18*, Vancouver, Canada, Apr.–May 2018, pp. 4819–4822.  
doi:10.18429/JACoW-IPAC2018-THPML074
- [11] K. Ohmi, *et al.*, “Electron Cloud Studies in SuperKEKB Phase I Commissioning”, in *Proc. IPAC’17*, Copenhagen, Denmark, May 2017, pp. 3104–3106.  
doi:10.18429/JACoW-IPAC2017-WEPIK075
- [12] H. Fukuma *et al.*, “Observation of vertical beam blow-up in KEKB low energy ring”, in *Proc. of EPAC’00*, Vienna, Austria, Jun. 2000, pp. 1122–1124, <https://accelconf.web.cern.ch/e00/PAPERS/WEP5A12.pdf>
- [13] L. Wang *et al.*, “Numerical study of the photoelectrons cloud in KEKB low energy ring with a three-dimensional particle in cell method”, *Phys. Rev. ST Accel. Beams*, vol. 5, p. 124402, 2002.  
doi:10.1103/PhysRevSTAB.5.124402
- [14] H. Fukuma *et al.*, “Status of Solenoid System to Suppress the Electron Cloud Effects at the KEKB”, in *AIP Conference Proceedings 642, ICFA-HB2002*, Batavia, USA, Apr. 2002, pp.357–359. doi:10.1063/1.1522668
- [15] S. S. Win *et al.*, “Numerical study of coupled-bunch instability caused by an electron cloud”, *Phys. Rev. ST Accel. Beams*, vol. 8, p. 094401, 2005.  
doi:10.1103/PhysRevSTAB.8.094401
- [16] G. Iadarola and G. Rumolo, “PyELOUD and build-up simulations at CERN”, in *Proc. ELOUD’12*, Isola d’Elba, Italy, Jun. 2012, CERN, Yellow Report No. CERN-2013-002, pp. 189–194., <https://ecloud12.web.cern.ch/Proceedings/Edited/Iadarola-edited.pdf>
- [17] Y. Suetsugu *et al.*, “R&D of copper beam duct with antechamber scheme for high current accelerators”, *Nucl. Instrum. Methods Phys. Res. A*, vol. 538, p. 206, 2005.  
doi:10.1016/j.nima.2004.09.015
- [18] K. Shibata *et al.*, “Development of TiN coating system for beam ducts of KEK B-factory”, in *Proc. EPAC’08*, Genoa, Italy, Jun. 2008, pp. 1700–1702, <https://accelconf.web.cern.ch/e08/papers/tupp071.pdf>
- [19] H. Fukuma, “Effect of Solenoid in Quadrupole Magnet on Electron Cloud Instability”, presented in *11<sup>th</sup> KEKB Review Committee*, KEK, Tsukuba, Japan, Mar. 2006, <https://www-kekb.kek.jp/MAC/2006/Report/>
- [20] H. Fukuma, private communication, Aug. 2022.
- [21] Y. Suetsugu *et al.*, “Continuing study on electron-cloud clearing techniques in high intensity positron ring: Mitigation by using groove surface in vertical magnetic field”, *Nucl. Instrum. Methods Phys. Res. A*, vol. 604, p. 449, 2009.  
doi:10.1016/j.nima.2009.03.011
- [22] Y. Suetsugu *et al.*, “Construction status of the SuperKEKB vacuum system”, *Vacuum*, vol. 121, p. 238, 2015.  
doi:10.1016/j.vacuum.2014.12.010
- [23] T. Hirai *et al.*, “Real-time luminosity monitor for a B-factory experiment”, *Nucl. Instrum. Methods Phys. Res. A*, vol. 458, p. 670, 2001. doi:10.1016/S0168-9002(00)00766-X
- [24] S. Uehara, private communication, July. 2022.
- [25] M. Yao *et al.*, “Study on copper thermal spray coating to mitigate electron cloud effect”, in *Proc. PASJ2021*, Online, Japan, Aug. 2021, paper TUP010, pp. 427–431.  
[https://www.pasj.jp/web\\_publish/pasj2021/proceedings/PDF/TUP0/TUP010.pdf](https://www.pasj.jp/web_publish/pasj2021/proceedings/PDF/TUP0/TUP010.pdf)